Approximation of single equivalent mobilities of timber joist floors

Andreas Mayr[a] and Barry Gibbs[b]

[a]Stuttgart University of Applied Sciences, Schellingstrasse 24, 70174 Stuttgart, Germany
[b]University of Liverpool, School of Architecture, Abercromby Square, L693BX Liverpool, UK
bmg@liv.ac.uk

To estimate the structure-borne sound power of vibrational active machines or components two source quantities, corresponding to the source activity and mobility, and one receiver quantity, the mobility, are usually required. A practical, laboratory-based measurement procedure for the characterisation of mechanical installations has recently been proposed, which yields single equivalent values of source strength and source mobility. In order to predict the power in the installed condition, an estimate of the receiver mobility also is required, again, for practical reasons, in the form of a single equivalent value. This paper considers the single equivalent receiver mobilities for lightweight building structures - timber joist floors. The value obtained is in the form of the average magnitude of the effective mobilities over the contact points. A simple prediction method is proposed for point- and transfer mobilities (both are required to yield the effective mobility at each contact) based on infinite beam and infinite plate behaviour. Estimates for point-, transfer- and single equivalent receiver mobilities are discussed and compared with measured data.

1 Introduction

Mechanical installations in buildings are often combined sources of airborne and structure-borne sound [1]. The structural dynamics of both the source and receiving systems are required for prediction of the structure-borne transmission in the installed condition. The transmission requires consideration of several contacts and up to six components of excitation at each contact. In the case of lightweight buildings, the magnitude of the receiver mobility and that of the source mobility can have the same value. The receiver mobility will vary significantly with location and the transmissions at the contacts may then differ greatly.

A laboratory-based measurement procedure for the characterisation of mechanical installations recently has been proposed [2], which yields single equivalent values of source strength and source mobility. In order to predict the power in the installed condition, an estimate of the receiver mobility also is required, again, for practical reasons, in the form of a single equivalent value.

This paper considers single equivalent receiver mobilities for lightweight building structures - timber joist floors. The value obtained is in the form of the average magnitude of the effective mobilities over the contact points. Since it is expected that this quantity will not be measurable in most cases, a simple prediction method is proposed for point- and transfer mobilities (both are required to yield the effective mobility at each contact) based on infinite beam and infinite plate behaviour. Estimates for point-, transfer- and single equivalent receiver mobilities are discussed and compared with measured data.

2 Timber joist floor

A timber joist floor was selected for this study because it represented a case where the spatial variation in point mobility is expected to be large. The floor, shown in Fig. 1, was constructed from 21 mm chipboard sheathing supported by seven Norwegian spruce joists 0.096 m x 0.192 m x 4.55 m, spaced 0.78 m on centre. The chipboard was in 0.9 m x 2.05 m panes, joined by tongue and grooves and secured to the joists using screws; no glue was used. The overall floor dimensions were 4.55 m x 4.95 m. A massive concrete test frame supported the ends of each joist without additional fixing and intermediate layer. No ceiling was installed.

It was assumed that sources might be fixed directly onto the joists or onto the bays between joists or in a combination of these two conditions. It was recognised that sources may be fixed with locating screws which do not penetrate to the joist below. Indeed, there are situations where sources rest on receiver structures without fixing.

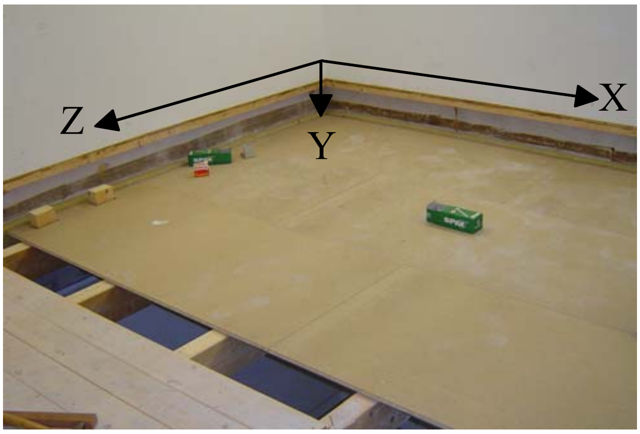

Fig.1 Wood joist floor

The point mobility was measured along a line perpendicular to the joists (x-direction in Fig. 1). Fig. 2 shows the measured point mobility normalized to that of an infinite plate and plotted as a function of distance in wavelengths. When the distance is less than one-quarter of the wavelength, joist behaviour dominates. At distances greater than one-quarter wavelength, the chipboard panel can be considered as an uncoupled infinite plate [3].

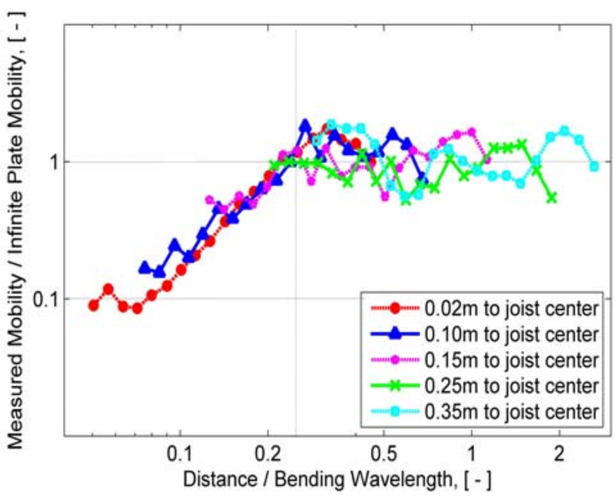

Fig.2 Point mobility as function of non-dimensional distance between the drive point and nearest joist.

To examine the effect of distance to the nearest screw point, the mobility for positions above a joist was recorded above and along a joist (z-direction in Fig. 1). In Fig. 3 again, the measured point mobility is normalized to that of an infinite plate and plotted as a function of the distance in wavelengths to the nearest screw. The behaviour observed in Figure 3 for distance from a screw is the same observed in Figure 2 for perpendicular distance from a joist.

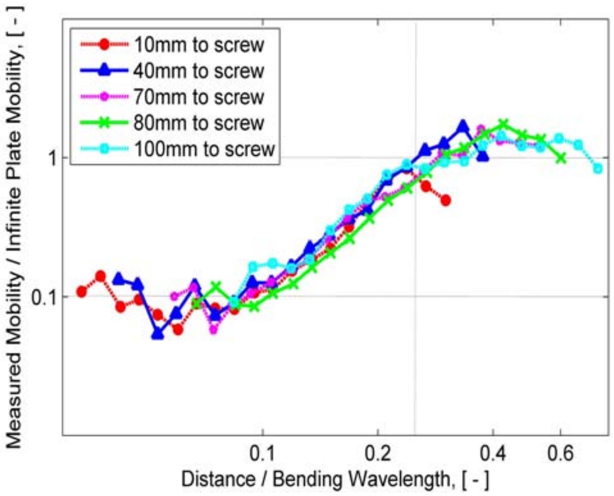

Fig.3 Point mobility as function of non-dimensional distance between the drive point and nearest fixing point

These similarities allow generalization. The distance, in wavelengths, between the observation point and the nearest screw is the determining factor. The infinite beam assumption applies for distances below 0.1 bending wave-length; the infinite plate assumption applies above 0.25 bending wavelength; between 0.1 and 0.25 straight-line interpolation applies. It remained to consider how these simple relationships could be predicted and incorporated into a single equivalent value for the receiving structure.

3 Single equivalent excitation

Machines and machine components are connected to supporting structures through multiple points, line and area contacts. The expression for total power is,

$$P_{SR}^{Total} = \frac{1}{2}\left(\{\overline{v}_{sf}\}^T \left[[\overline{Y}_S] + [\overline{Y}_R]^T \right]^{-1} Re([\overline{Y}_R]) \left[[\overline{Y}_S^*] + [\overline{Y}_R^*] \right]^{-1} \{\overline{v}_{sf}^*\} \right) \tag{1}$$

$\{\overline{v}_{sf}\}$ is the complex free velocity vector and $[\overline{Y}_S],[\overline{Y}_R]$ the complex mobility matrices of size N x N, where N is the number of contacts. In this study, forces perpendicular to the receiver structure only are considered.

As a first step to deriving a single equivalent formulation, it is possible to re-express equation (1) by reference to the concept of the effective mobility [4]. The total power, from a source S to a receiver R, through all contacts is,

$$P_{SR}^{Total} = \frac{1}{2}\sum_i^N |\overline{v}_{sfi}|^2 \frac{Re(\overline{Y}^{\Sigma}{}_{Ri})}{|\overline{Y}^{\Sigma}{}_{Si} + \overline{Y}^{\Sigma}{}_{Ri}|^2} \tag{2}$$

For both the source and receiver, the effective point mobility at the i^{th} contact is,

$$\overline{Y}_i^{\Sigma} = \overline{Y}_i + \sum \frac{\overline{F}_j}{\overline{F}_i}\overline{Y}_{i,j} \tag{3}$$

$\overline{Y}_i$ is the point mobility at the i^{th} contact, $\overline{Y}_{i,j}$ is the transfer mobility between the i^{th} and j^{th} contacts and $\frac{\overline{F}_j}{\overline{F}_i}$ is the ratio of the forces at the j^{th} and i^{th} contact, respectively. The complex force ratio is not likely to be known and simplifying assumptions are necessary [5]. The forces can be assumed to be of equal magnitude. The phase difference between forces depends on the vibration behaviour of the source. If a zero phase difference is assumed, then equation (3) becomes,

$$\overline{Y}_i^{\Sigma} \approx \overline{Y}_i + \sum \overline{Y}_{i,j} \tag{4}$$

If a random phase is assumed then,

$$|\overline{Y}_i^{\Sigma}|^2 \approx |\overline{Y}_i|^2 + \sum |\overline{Y}_{i,j}|^2$$

and

$$\mathrm{Re}(\overline{Y}_i^{\Sigma}) \approx \mathrm{Re}(\overline{Y}_i) \tag{5}$$

Therefore, the two source quantities and the one receiver quantity, required for prediction of the installed power, can be expressed as single equivalent values. The first source quantity, from equation (2), is the sum of the squares of the magnitudes of complex free velocities at the source contacts $\sum_i^N |\overline{v}_{sfi}|^2$. The second source quantity is the single equivalent source mobility, which is the average complex effective source mobility over the contacts, $\overline{Y}_S^{\Sigma} = \frac{1}{N}\sum_i^N \overline{Y}_i^{\Sigma}$.

This can be measured directly or obtained indirectly by a simple reception plate method, but only as the magnitude of the mean effective mobility $|\overline{Y}_S^{\Sigma}|$ [2]. It is demonstrated that these real-value quantities are appropriate for prediction of installed power for a range of source-receiver mobility conditions [6,7]. The above discussion leads to the associated single equivalent receiver mobility and how it can be obtained.

4 Measured receiver mobility

The timber joist floor, described earlier, was used to obtain the single equivalent receiver mobility for various source locations indicated in Fig. 4.

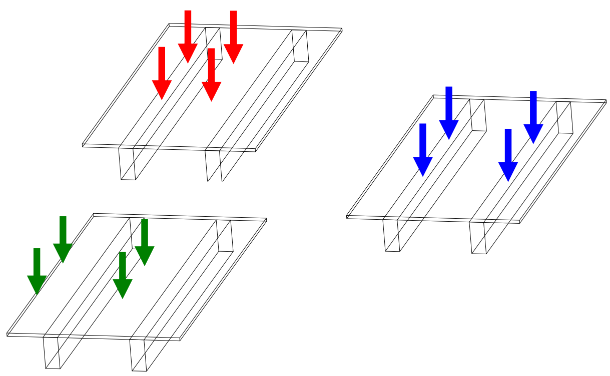
Fig.4 Different mounting conditions

Again, the timber joist floor was selected since large spatial variations in receiver mobility were expected, depending on if the source contacts are over a joist, between joists or if there is a mix of contact conditions.

Fig. 5 shows measured single equivalent receiver mobility for assumed mounting conditions according to Fig. 4. When the source is assumed to have a higher mobility than the receiver (force source situation), the equivalent receiver mobilities show plate-like dynamic behaviour, although two points are located on a joist.

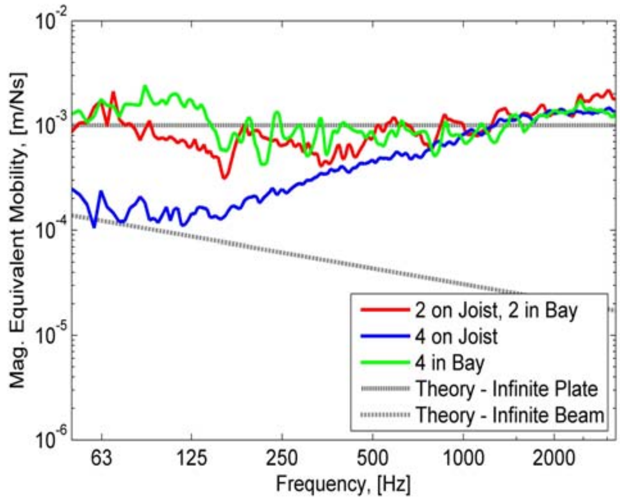

Fig.5 Equivalent single receiver mobilities of timber joist floor for different mounting conditions

However, there will be situations, e.g. rigidly fixing a source with all contacts to a joist, where the equivalent receiver mobilities indicate beam-like behaviour, at least in the low frequencies as shown. When the source is assumed to have a lower mobility than the receiver (velocity source situation), the single equivalent receiver mobility is obtained by summing impedances rather than mobilities in order to account for lower joist mobilities,

$$\overline{Y}_{eq}^{\Sigma} = \left[\frac{1}{N}\sum_{i}^{N}\left(\overline{Y}_{i}^{\Sigma}\right)^{-1}\right]^{-1} \qquad (6)$$

5 Predicted receiver mobility

Again, the regular and repeatable dynamic behaviour of the floor, indicated in Fig. 5, points to a simple prediction method for point- and transfer mobility, and thence single equivalent receiver mobility. The approach is based on considering the reactive forces at the screw points, which result from the forces generated at the contacts between source and receiver [8].

5.1 Point mobility

The plate response velocities and forces (Fig. 6) are given as

$$\begin{Bmatrix} v_i \\ v_{r_n} \end{Bmatrix} = \begin{bmatrix} Y_{i,i} & Y_{i,r_n} \\ Y_{r_n,i} & Y_{r_n,r_n} \end{bmatrix} \begin{Bmatrix} f_i \\ -f_{r_n} \end{Bmatrix} \qquad (7)$$

where f_{r_n} are the reactive forces at the screw points. The first row of eq. (7) describes the excitation point, the second row the contact points.

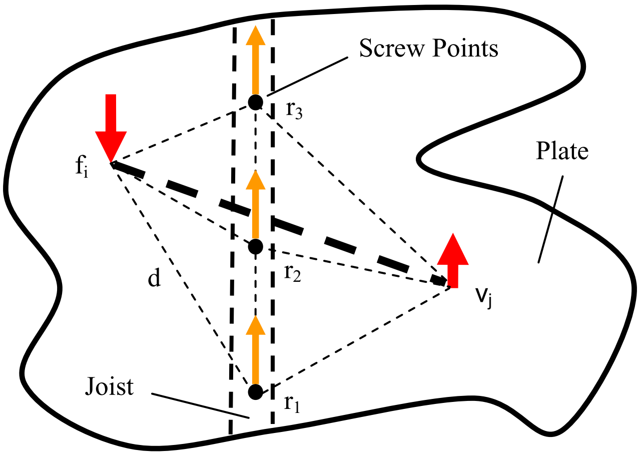

Fig. 6 Scheme of floor set-up used to predict point- and transfer mobilities of timber joist floor

The forces and velocities at the joist are given by

$$\left\{v_{Br_n}\right\} = \left[Y_B\right]\left\{f_{Br_n}\right\} \qquad (8)$$

where Y_B is the characteristic beam mobility matrix.

From eq. (7) and (8) and from continuity and equilibrium conditions: $v_{Br_n} = v_{r_n}$; $f_{Br_n} = f_{r_n}$

$$\begin{Bmatrix} v_i \\ v_{r_n} \end{Bmatrix} = \begin{bmatrix} Y_{i,i} & Y_{i,r_n} \\ Y_{r_n,i} & Y_{r_n,r_n} \end{bmatrix} \begin{Bmatrix} f_i \\ -Y_B^{-1} v_{r_n} \end{Bmatrix} \qquad (9)$$

v_i can be expressed in terms of f_i as

$$v_i = Y_{i,i}\, f_i - Y_{i,r_n}\left[Y_{r_n,r_n} + Y_B\right]^{-1} Y_{r_n,i}\, f_i \qquad (10)$$

and the point mobility at position *i* is given

$$Y'_{i,i} = Y_{i,i} - Y_{i,r_n}\left[Y_{r_n,r_n} + Y_B\right]^{-1} Y_{r_n,i} \qquad (11)$$

With $Y_{i,i}$ the uncoupled point mobility, Y_{i,r_n} the transfer mobilities from excitation point to contact points, $Y_{r_n,i}$ the transfer mobilities from contact points to excitation point, Y_B the "point" mobility matrix of beam at contact points, Y_{r_n,r_n} the point- and transfer mobility matrix of plate at contact points. The excitation and response points can be anywhere and the following assumptions are used:

$Y_{j,i} = Y_c\,\Pi_{j,i}$, $Y_{j,r_n} = Y_c\,\Pi_{j,r_n}$;

Y_B / Y_c = characteristic beam / -plate mobility;

$Y_{r_n,r_n} = Y_c\,\Pi_{r_n,r_n}$ and $Y_{r_n,i} = Y_c\,\Pi_{r_n,i}$;

with the propagation function:

$$\Pi(kd) = H_0^{(2)}(kd) - H_0^{(2)}(-jkd)$$

where $H_0^{(2)}$ is the second-order Hankel function, k the bending wave number and d the corresponding distances. These assumptions imply that only basic material properties and dimensions are required.

In Fig. 7 is shown the predicted and measured point mobility, 80 mm distant from the nearest screw position.

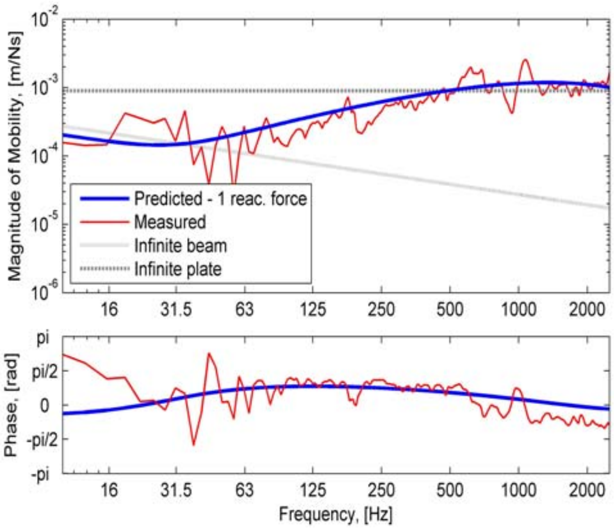

Fig. 7 Predicted and measured magnitude and phase of the point mobility 80 mm from the nearest screw position

With some manipulation, the contribution i.e. reactive forces of three additional screw positions were included and the results are shown in Fig. 8. The agreement between prediction and measurement is little improved, if at all, and an acceptable prediction is obtained from consideration of the simplest case of one screw point.

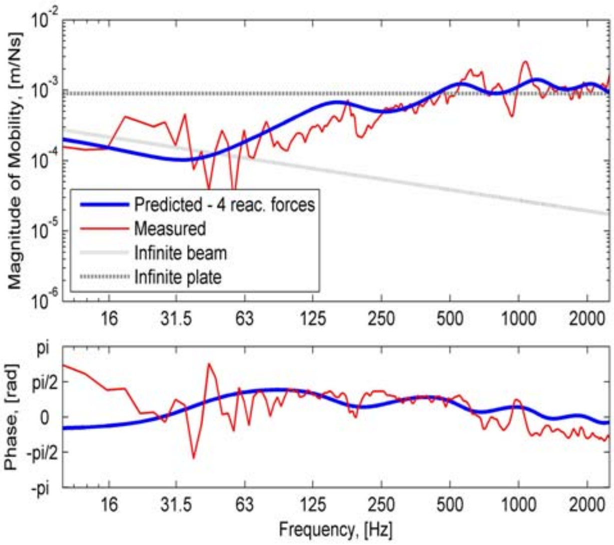

Fig. 8 Predicted and measured magnitude and phase of point mobility 80 mm from the nearest screw position; including the next three closest screw positions

5.2 Transfer mobility

The method described can be extended to predict transfer mobility (see Fig. 6) by the addition of an extra line for v_j

$$\begin{Bmatrix} v_i \\ v_j \\ v_{r_n} \end{Bmatrix} = \begin{bmatrix} Y_{i,i} & Y_{i,j} & Y_{i,r_n} \\ Y_{j,i} & Y_{j,j} & Y_{j,r_n} \\ Y_{r_n,i} & Y_{r_n,j} & Y_{r_n,r_n} \end{bmatrix} \begin{Bmatrix} f_i \\ 0 \\ -f_{r_n} \end{Bmatrix} \quad (12)$$

The transfer mobility follows

$$Y'_{j,i} = Y_{j,i} - Y_{j,r_n} \left[Y_{r_n,r_n} + Y_B \right]^{-1} Y_{r_n,i} \quad (13)$$

The predicted and measured transfer mobility is shown for two contact points midway between joists (in a bay), across one joist. The distance between points is 1.02 m. Two screw positions, and therefore two reactive forces, were considered. The agreement is promising, in terms of magnitude. There is agreement in terms of phase at low frequencies although there is under-prediction at frequencies above 125 Hz. As with point mobility prediction, additional screw points were considered but there was little or no improvement in agreement and these results are not shown. It was observed that transfer mobility predictions are sensitive to small changes in distance, both from the source to the screw and from the screw to the response position. The method of reactive forces is equally applicable to point and transfer mobility estimates and equally accurate (compare Fig. 8 and Fig. 9). The transfer mobility across a joist is significantly lower in magnitude than that of the associated point mobilities at mid and high frequencies, in this case in the frequency range 125 Hz – 2.5 kHz. At low frequencies, and for compatible distances, transfer mobility terms will need to be included when assembling the associated single equivalent mobility

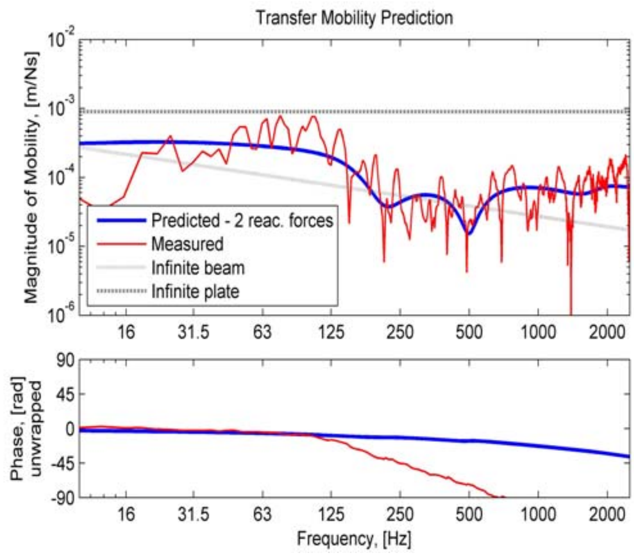

Fig. 9 Predicted and measured magnitude and phase of transfer mobility between bays separated by a joist.

5.3 Single equivalent mobility

From previous measurements of point and transfer mobilities, single equivalent receiver mobilities were calculated for two different sources and various contact conditions [6]. The case considered is for a fan unit on four mounts when two feet are on a joist and two feet are in a bay. In general, the spatial variation for different mounting situations is not large and adds credibility to the concept of a single equivalent value.

In Fig. 10 the associated predicted equivalent values are shown for the case using the complex force ratio (see eq. 3) obtained from measured free velocity and measured source- and receiver mobilities. The discrepancy is due to the spatial variation in contact force, which appears to be sufficiently small to allow the assumption of a single equivalent value and the agreement is acceptable overall.

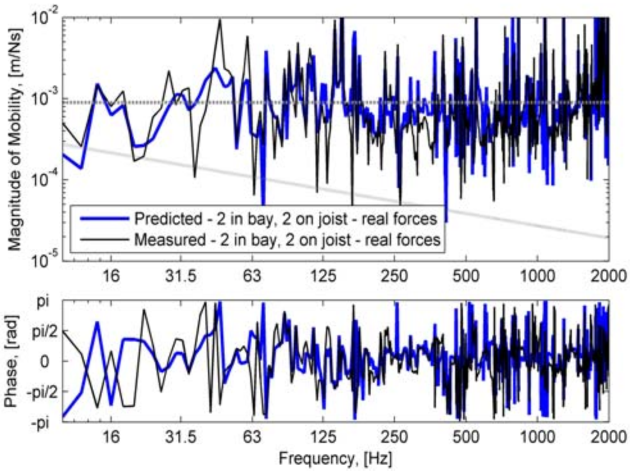

Fig. 10 Predicted and measured magnitude and phase of single equivalent receiver mobility using measured complex force ratio

Since the complex force ratio is not likely to be known, simplifying assumptions are necessary and the forces can be assumed to be of equal magnitude.

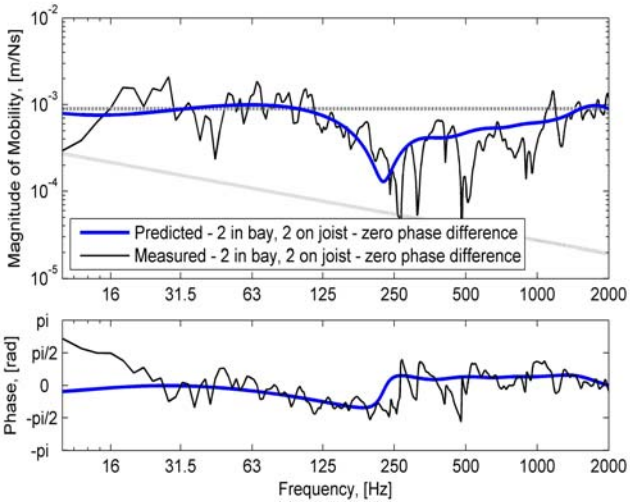

Fig. 11 Predicted and measured magnitude and phase of single equivalent receiver mobility assuming unit force ratio and zero phase difference

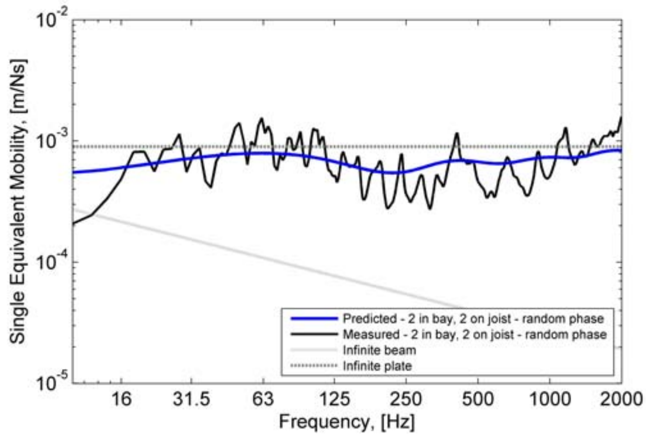

Fig. 12 Predicted and measured magnitude of single equivalent receiver mobility assuming unit force ratio and random phase difference

If a zero phase difference is assumed, the complex single equivalent values are calculated according to eq. 4 and shown in Fig. 11. If a random difference is assumed, then the magnitude is obtained according to eq. 5 and is shown in Fig. 12. The real part of the single equivalent receiver mobility is obtained from the average of the complex point mobilities, again according to eq. 5.

6 Conclusion

The receiver mobility of ribbed timber floors can be predicted in terms of characteristic plate and beam mobilities. Both the point and transfer mobilities obtained can be used for prediction of structure-borne sound transmission at each contact, if the associated source data is available.

Alternatively, a predicted single equivalent receiver mobility can be assembled for use with the associated single equivalent source mobility.

Acknowledgments

The authors gratefully acknowledge the financial support provided by EPSRC, UK and the collaborative work on this study with Professor Heinz-Martin Fischer of Stuttgart University of Applied Sciences and Dr. Andrew Moorhouse of Salford University Acoustics Research Centre.

References

[1] EN12354: Estimation of acoustic performance of building from the performance of elements – Part 5: Sound levels due to service equipment

[2] B. M. Gibbs, N. Qi, A. T. Moorhouse, “A practical characterization for vibro-acoustic sources in buildings” *Acta Acustica u.with Acustica*, 93, 84-93 (2007).

[3] A. R. Mayr, T. R. T. Nightingale, “On the mobility of joist floors and periodic rib-stiffened plates”, *Proceedings Inter-Noise*, Istanbul, Turkey (2007).

[4] B. A. T. Petersson, J. Plunt, “On effective mobilities in the prediction of structure-borne sound transmission between a source and a receiving structure”, *Journal of Sound and Vibration* 82 (4), 517-529 (1982).

[5] R. A. Fulford, B. M. Gibbs, “Structure-borne sound power and source characterisation in multi-point-connected systems, Part1: Case studies for assumed force distributions”, *JSV* 204(4), 659-677 (1997).

[6] B. M. Gibbs, A. R. Mayr, “Structure-borne sound from machines in lightweight buildings”, *Proceedings ICSV 15*, Daejeon, Korea (2008)

[7] B. M. Gibbs, A. R. Mayr, “A structure-borne sound source characterization based on single equivalent values”, *Proceedings. Acoustics 08*, Paris (2008)

[8] R. Tschakert, B. A. T. Petersson, “The attenuation of structure-borne sound in non-periodically stiffened plates”, *Proceedings ICA 19th*, Madrid, Spain (2007)